Heterogeneous Reactions of Isoprene-Derived Epoxides: Reaction Probabilities and Molar Secondary Organic Aerosol Yield Estimates

Theran P. Riedel,[†] Ying-Hsuan Lin,[†] Sri Hapsari Budisulistiorini,[†] Cassandra J. Gaston,[‡] Joel A. Thornton,[‡] Zhenfa Zhang,[†] William Vizuete,[†] Avram Gold,[†] and Jason D. Surratt*,[†]

[†]Department of Environmental Sciences and Engineering, Gillings School of Global Public Health, The University of North Carolina at Chapel Hill, Chapel Hill, North Carolina 27599, United States

[‡]Department of Atmospheric Sciences, University of Washington, Seattle, Washington 98195-1640, United States

S Supporting Information

ABSTRACT: A combination of flow reactor studies and chamber modeling is used to constrain two uncertain parameters central to the formation of secondary organic aerosol (SOA) from isoprene-derived epoxides: (1) the rate of heterogeneous uptake of epoxide to the particle phase and (2) the molar fraction of epoxide reactively taken up that contributes to SOA, the SOA yield (ϕ_{SOA}). Flow reactor measurements of the *trans-β*-isoprene epoxydiol (*trans-β*-IEPOX) and methacrylic acid epoxide (MAE) aerosol reaction probability (γ) were performed on atomized aerosols with compositions similar to those used in chamber studies. Observed γ ranges for *trans-β*-IEPOX and MAE were 6.5×10^{-4}–0.021 and 4.9–5.2×10^{-4}, respectively. Through the use of a time-dependent chemical box model initialized with chamber conditions and γ measurements, ϕ_{SOA} values for *trans-β*-IEPOX and MAE on different aerosol compositions were estimated between 0.03–0.21 and 0.07–0.25, respectively, with the MAE ϕ_{SOA} showing more uncertainty.
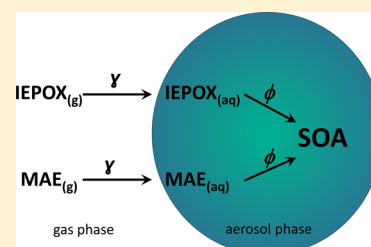
INTRODUCTION

Isoprene, the most abundant non-methane hydrocarbon in the atmosphere, has large potential effects on air quality and radiative forcing.[1] Formation of secondary organic aerosol (SOA) from photochemical oxidation of isoprene represents a significant source of fine aerosol mass (PM$_{2.5}$),[2,3] especially in the southeastern United States during the summer.[4−6] Epoxides formed from isoprene oxidation have been shown to be critical precursors of isoprene-derived SOA.[7,8] Isoprene epoxydiols (IEPOX) and methacrylic acid epoxide (MAE) have the capability of producing SOA through reactive uptake to atmospheric PM$_{2.5}$.[6] Subsequent condensed-phase reactions form "tracer" species (organosulfates, 2-methyltetrols, C$_5$-alkene triols, and 2-methylglyceric acid) that contribute to the SOA burden.[8−10] Ambient mixing ratios of isoprene-derived epoxides have been observed in excess of 3 ppbv for IEPOX and 50 pptv for MAE.[7,8]

Heterogeneous reactions of these epoxides leading to SOA formation remain poorly constrained. Direct measurements of the heterogeneous uptake rate, often reported as the gas−aerosol reaction probability or reactive uptake coefficient (γ), have only recently begun.[11] γ is the number of gas-phase molecules removed by the aerosol phase per total number of gas−aerosol collisions. This parameter is convenient for modeling heterogeneous reactions as it can be efficiently incorporated into regional and global models.[12,13] Most epoxide γ estimates to this point have relied on indirect parametrizations based on Henry's law and aqueous rates of epoxide reactions in macroscopic solutions.[12,14]

Of equal importance to γ in terms of SOA production is the molar fraction of epoxide that, once accommodated to the aerosol phase, produces the SOA mass − the SOA molar yield (ϕ_{SOA}). ϕ_{SOA} is defined as the sum of the rates of all aqueous-phase SOA tracer formation reactions relative to the heterogeneous rate of gas-phase epoxide loss to particles, illustrated by eq 1.

$$\phi_{SOA} = \frac{\sum_{i=1}^{n} k_i [\text{epoxide}]_{(aq)}}{k_{het} [\text{epoxide}]_{(g)}} \quad (1)$$

Traditionally, epoxide SOA production studies have reported estimates of the SOA mass yield, an equilibrium parameter calculated as the mass of SOA produced relative to the quantity of epoxide consumed or injected into the chamber.[9,10] The mass yield can be roughly related to ϕ_{SOA}, provided the mass fractions and molecular weights of all formed SOA tracers are known.

Here we investigate the molar extent to which *trans-β*-IEPOX, the predominant isomer of IEPOX,[15] and MAE lost to heterogeneous reactions contribute to SOA.

METHODS

Epoxide Uptake Measurements. Similar to previous publications,[11,16,17] we used entrained gas−aerosol flow reactor

techniques to determine γ. γ for *trans-β*-IEPOX and MAE were measured using a cylindrical glass flow reactor (1 m in length × 8 cm inner diameter) coated with halocarbon wax (Halocarbon Products Corp.) to minimize wall loss reactions.

Aerosols were generated using a custom-built atomizer that outputs polydisperse aerosol into a nitrogen carrier flow at ~2 standard liters per minute (slpm). Atomizer solutions were chosen to match the seed aerosol of SOA chamber studies that showed significant SOA growth (described below). Atomized aerosol was mixed with a nitrogen dilution flow of ~3 slpm and injected into the flow reactor through a top side port perpendicular to the flow axis. Depending on the desired relative humidity (RH), the aerosol stream was directed through a diffusion dryer (TSI Inc.) and the dilution flow through a water bubbler prior to entering the reactor.

trans-β-IEPOX and MAE were delivered to the reactor by passing ~0.1 slpm of nitrogen over a 20 μg/mL epoxide solution in ethyl acetate. Synthetic procedures for generating authentic *trans-β*-IEPOX and MAE have been published elsewhere.[8,18] Epoxide was introduced into the aerosol stream through an injector rod inserted axially down the center of the reactor. The injector was moved along the length of the reactor to control the epoxide−aerosol interaction time. At the base of the reactor, submicrometer (10−850 nm) aerosol number size distributions were measured through a perpendicular port using a scanning electrical mobility system (SEMS) with a differential mobility analyzer [<25% RH sheath flow] and a mixing condensation particle counter (Brechtel Inc.). The aerosol number distributions were converted to total surface area concentrations (S_a) which ranged from 18000 to 65000 μm^2/cm^3 for individual experiments. Epoxide levels were monitored through another perpendicular port using a time-of-flight chemical ionization mass spectrometer (Aerodyne Research, Inc.) with both acetate and iodide reagent ion chemistries.[19,20] γ estimates were consistent between the two reagent ions. Flow reactor RH was also measured at the base with a commercial RH−temperature sensor (Omega Engineering Inc.).

The heterogeneous pseudo-first-order rate coefficient (k_{het}) for the uptake of epoxide to aerosols was measured by moving the epoxide injector between six positions along the length of the reactor. A linear fit of the averaged natural logarithm of the epoxide signal at each injector position versus reaction time yielded a slope equal to the sum of k_{het} and the loss rate coefficient of epoxide on the reactor walls ($k_{total} = k_{het} + k_{wall}$). The slope of a linear fit of a second decay performed at the same RH in the absence of aerosols yielded k_{wall} (typically <0.01 s^{-1}). Figure 1 shows a normalized time decay and the associated linear fit for both *trans-β*-IEPOX and MAE with and without aerosols present. Assuming plug flow conditions, the difference between k_{total} and k_{wall} is k_{het}. In practice, however, an iterative correction for non-plug flow conditions was applied,[21] and k_{het} was then converted to γ using eq 2

$$\gamma = \frac{4k_{het}}{S_a\omega} \tag{2}$$

where ω is the mean molecular speed of an epoxide molecule (231 m/s for *trans-β*-IEPOX and 249 m/s for MAE at 298 K). A minimum of three γ measurements was used for all reported γ averages and 1σ uncertainties.

Epoxide SOA Chamber Experiments. *trans-β*-IEPOX and MAE chamber studies were performed to assess SOA growth with various RH and seed aerosol types. A complete
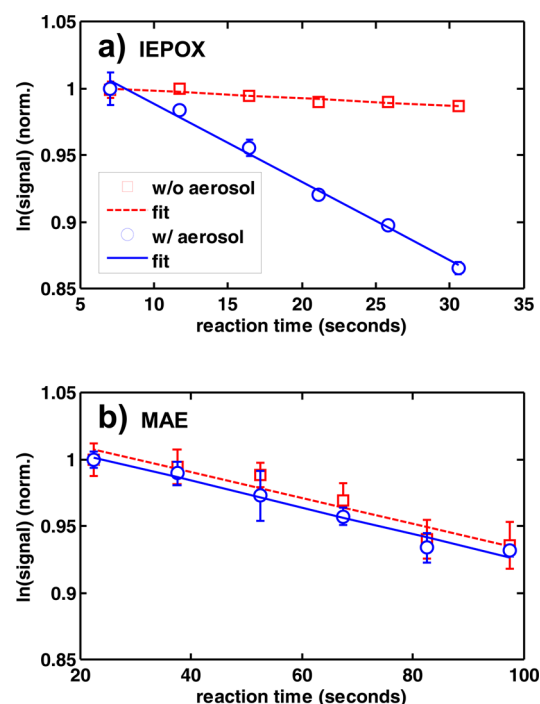

Figure 1. Average of the logarithm of the epoxide signal vs reaction time and associated linear fit without aerosols (red squares, $\pm2\sigma$; red dashed line) and with aerosols present in the flow reactor (blue circles, $\pm2\sigma$; blue solid line) for (a) *trans-β*-IEPOX and (b) MAE on a $(NH_4)_2SO_4 + H_2SO_4$ aerosol. Initial values have been normalized to 1 for ease of comparison.

description of the chamber experiments can be found elsewhere.[8,10] Briefly, *trans-β*-IEPOX or MAE was injected into a dry (~5% RH) or humidified (~50% RH) 10 m^3 Teflon chamber that was prefilled with ~35 μg/m^3 of inorganic seed aerosol as measured by SEMS or a scanning mobility particle sizer with a differential mobility analyzer and a condensation particle counter (TSI Inc.). Seed aerosol was generated by atomizing one of three solutions: 0.06 M $(NH_4)_2SO_4$, 0.06 M $(NH_4)_2SO_4$ + 0.06 M H_2SO_4, or 0.06 M $MgSO_4$ + 0.06 M H_2SO_4. Fifteen milligrams of *trans-β*-IEPOX or MAE standard was delivered to the seeded chamber by passing 5 slpm N_2 through a glass manifold heated at 60 °C for 1−2 h until the SOA mass concentration had stabilized. The injection efficiency through the manifold was estimated to be 0.74 ± 0.13 (1σ) from mass measurements of the manifold before and after injections from multiple ($n = 10$) chamber experiments.

■ RESULTS AND DISCUSSION

Flow Reactor Measurements of γ. Table 1 summarizes γ results for *trans-β*-IEPOX and MAE, including the 1σ error for each measurement. As stated above, aerosol and RH conditions chosen for the flow reactor were representative of conditions that produced observable SOA growth in the chamber experiments. Table 1 also includes estimates of aerosol acidity obtained from the Extended AIM Aerosol Thermodynamics Model III (http://www.aim.env.uea.ac.uk/aim/aim.php)[22,23] using atomizer solution composition and chamber RH as inputs (see Supporting Information). The highest γ for *trans-β*-IEPOX ($\gamma = 0.021$) was observed for the $(NH_4)_2SO_4 + H_2SO_4$ seed aerosol under dry conditions. γ values were similar to previous measurements for *trans-β*-IEPOX, showing a general increase in γ with higher aerosol acidity,[11] consistent with

Table 1. Summary of Experiments and Results

epoxide	aerosol	RH	aerosol [H$^+$] (M)^a	$\gamma \pm 1\sigma$	chamber SOA mass yield	modeled ϕ_{SOA} range
IEPOX	(NH$_4$)$_2$SO$_4$	0.50	7.74×10^{-5}	$(6.5 \pm 6.4) \times 10^{-4}$	0.04	0.17−0.21
IEPOX	MgSO$_4$ + H$_2$SO$_4$	0.08	0.04	$(1.1 \pm 0.3) \times 10^{-2}$	0.08	0.04−0.06
IEPOX	MgSO$_4$ + H$_2$SO$_4$	0.53	0.73	$(9.4 \pm 3) \times 10^{-3}$	0.04	0.03−0.05
IEPOX	(NH$_4$)$_2$SO$_4$ + H$_2$SO$_4$	0.05	2.78	$(2.1 \pm 0.1) \times 10^{-2}$	0.10	0.10−0.12
IEPOX	(NH$_4$)$_2$SO$_4$ + H$_2$SO$_4$	0.59	2.01	$(1.9 \pm 0.2) \times 10^{-2}$	0.06	0.06−0.08
MAE	MgSO$_4$ + H$_2$SO$_4$	0.03	0.73	$(4.9 \pm 1) \times 10^{-4}$	0.01	0.07−0.14
MAE	(NH$_4$)$_2$SO$_4$ + H$_2$SO$_4$	0.03	2.78	$(5.2 \pm 1.1) \times 10^{-4}$	0.01	0.16−0.25

^{a}Estimated from an E-AIM model calculation moles of H$^+$ and the total volume of the aqueous phase. E-AIM RH input must be ≥0.1, so the same [H$^+$] is estimated for similar aerosol compositions despite differences in experimental RH.

particle-phase acid-catalyzed epoxide reactions.[24,25] A decrease in γ observed for the same aerosol type at higher RH can likely be attributed to dilution of acidity by additional aerosol water.[11] For MAE, γ values were ∼30-fold smaller than for trans-β-IEPOX, consistent with MAE acid-catalyzed reaction rate constants being ∼600-fold lower than those of trans-β-IEPOX.[26] These differences may in part be responsible for the smaller observed SOA production from MAE compared to IEPOX.[6] Only at acidities closer to neutral ([H$^+$] ≈ 8 × 10^{-5} M) do the γ values of trans-β-IEPOX approach those of MAE (γ ≈ 5 × 10^{-4}). The apparent convergence most likely results from values of γ approaching detection limits, so the γ values of trans-β-IEPOX and MAE at low aerosol acidity likely differ and are potentially smaller than those reported here.

Chamber Box Modeling of ϕ_{SOA}. Atomizer solutions and RHs used in the flow reactor studies were chosen to match those of the chamber studies. Thus, γ measured in the flow reactor experiments captured the γ expected for the chamber experiments and provided a reliable constraint on chamber epoxide uptake rates. To properly assess overall SOA production, however, ϕ_{SOA} is also needed. A 0-D time-dependent box model was used to simulate the chamber experiments and estimate ϕ_{SOA}. The model was initialized with γ values from the flow reactor measurements (and therefore subject to similar uncertainties), the amount of epoxide injected into the chamber scaled by the estimated injection efficiency, chamber-measured S_a and mass concentrations (assuming an aerosol density of 1 g/mL), the estimated epoxide and aerosol chamber wall loss rates from epoxide injections in the absence of seed particles and aerosol seed only injections at the appropriate RH, and ϕ_{SOA} values chosen to bracket chamber-measured aerosol mass loadings. The wall loss estimates do not take into account non-first-order epoxide losses (e.g., reversible wall losses, changes in wall loss with aerosols present, particle-to-wall partitioning of tracer species), which could affect SOA production. Chemical rate equations for gas- and aerosol-phase epoxide were integrated over the duration of the chamber experiment to determine time-dependent concentrations. The only modeled losses of gas-phase epoxide were to S_a and chamber walls, and the only modeled source of aerosol-phase epoxide was the reaction of gas-phase epoxide on S_a scaled by ϕ_{SOA}.

S_a was held constant over model runs, although SOA formation contributes to the S_a. Given the modest SOA growth for MAE, this approximation is less of an issue than for trans-β-IEPOX. For trans-β-IEPOX, additional SOA resulted in at most a 40% increase in S_a. It is unclear how this additional S_a would affect the modeled SOA growth. It could result in an increase in γ if the SOA component of the aerosol was as efficient at uptake as the inorganic phase. However, previous studies show that the

presence of aerosol-phase semioxidized organics in the form of polyethylene glycol tended to inhibit trans-β-IEPOX uptake, thereby slowing SOA growth.[11] Indeed, the modeled SOA growth rate tended to be faster than that observed in the chamber experiments, although this effect could be in part a result of the instantaneous mixing assumed by the box model.

Choosing ϕ_{SOA} values to bracket the observed chamber SOA mass growth yields an upper and lower estimate of ϕ_{SOA} (Figure 2). The ranges are reported in Table 1 along with
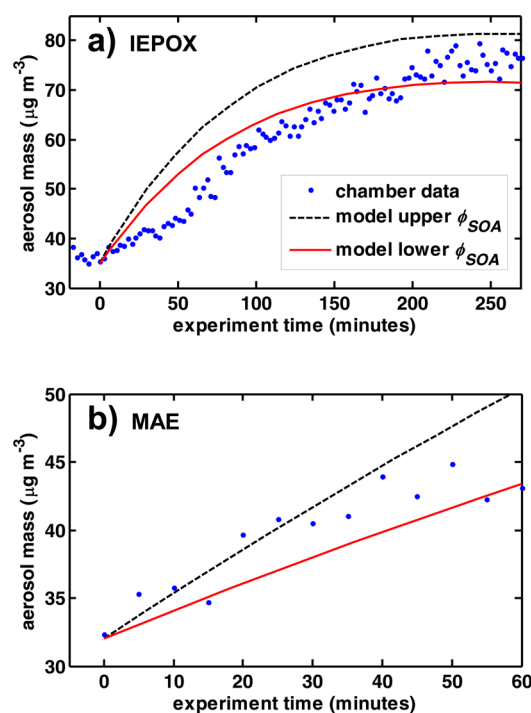

Figure 2. Chamber-measured (blue dots) and modeled (black dashed line, red solid line) SOA mass loadings for (a) trans-β-IEPOX with (NH$_4$)$_2$SO$_4$ seed and (b) MAE with (NH$_4$)$_2$SO$_4$ + H$_2$SO$_4$ seed. The black dashed lines represent an upper estimate of the molar SOA yield (ϕ_{SOA}), and the red solid lines represent a lower estimate (Table 1).

the SOA mass yields from the chamber experiments. For the different aerosol compositions, ϕ_{SOA} for trans-β-IEPOX varied from 0.03 to 0.21 and for MAE from 0.07 to 0.25, with slightly larger ϕ_{SOA} calculated for (NH$_4$)$_2$SO$_4$ seed. Aerosol conditions that influence γ—high aerosol acidity, the concentration of general acids like bisulfate, and the concentrations of nucleophiles—would in general be expected to influence ϕ_{SOA} similarly. While γ was largest for acidified aerosols, ϕ_{SOA} seems to be largely independent of acidity with the highest ϕ_{SOA} for trans-β-IEPOX (ϕ_{SOA} = 0.21) observed on the

nonacidified aqueous ammonium sulfate aerosol. Therefore, it appears that even in the absence of a high acid concentration, similar total SOA mass production can be achieved over a sufficiently long reaction time. Model outputs for *trans-β*-IEPOX showed good agreement with chamber observations, particularly the characteristic leveling off of the SOA mass growth (Figure 2a). MAE model outputs (Figure 2b) fail to capture the leveling off in aerosol mass, suggesting ϕ_{SOA} estimates for MAE may be less robust than those for *trans-β*-IEPOX. An underestimate of γ (corresponding ϕ_{SOA} over-estimate) or an underestimate of wall loss (corresponding ϕ_{SOA} underestimate) could result in this discrepancy between the model and measurements. Given the reproducibility of the γ measurements, we are inclined to attribute these differences to the latter, causing a low bias in calculated MAE ϕ_{SOA} (see Supporting Information).[27,28] That said, modest SOA growth coupled with the low time resolution of the mass concentration data makes modeling the MAE experiments inherently more difficult.

In the calculation of ϕ_{SOA}, the molecular weight of the SOA was estimated as the molecular weight of the epoxide consumed. However, many SOA tracers have molecular weights higher than those of the parent epoxides.[8,10] ϕ_{SOA} values reported here are thus likely to have a high bias. As a limiting example, the molecular weight of IEPOX-derived organosulfate (216 g/mol), a primary component of isoprene-derived SOA, is almost twice that of *trans-β*-IEPOX (118 g/mol). Assuming the SOA mass is entirely composed of organosulfates, ϕ_{SOA} for *trans-β*-IEPOX would be overestimated by ∼50%. This bias would likely offset to some degree a potential low bias resulting from epoxide wall losses or products that are not adequately captured.

As discussed above, it is unclear how γ and ϕ_{SOA} are affected when a significant fraction of S_a is represented by epoxide-derived SOA. This warrants further investigation as it could be relevant in regions like the southeastern United States during the summer where isoprene SOA can account for a substantial portion of $PM_{2.5}$ mass and therefore S_a. The results presented here, and in our previous study,[11] which constrain all reactions contributing to IEPOX- and MAE-derived SOA, could be beneficial for regional and/or global models to help constrain predictions of IEPOX- and MAE-derived SOA, especially because only a few known aqueous-phase reaction rates constrain current models.

■ ASSOCIATED CONTENT

Ⓢ Supporting Information

Flow reactor and chamber experiment details, aerosol model and wall loss assessments. This material is available free of charge via the Internet at http://pubs.acs.org.

■ AUTHOR INFORMATION

Corresponding Author

*E-mail: surratt@unc.edu. Phone: (919) 966-0470. Fax: (919) 966-7911.

Notes

The authors declare no competing financial interest.

■ ACKNOWLEDGMENTS

■ REFERENCES

(1) Guenther, A.; Karl, T.; Harley, P.; Wiedinmyer, C.; Palmer, P. I.; Geron, C. Estimates of global terrestrial isoprene emissions using MEGAN (Model of Emissions of Gases and Aerosols from Nature). *Atmos. Chem. Phys.* **2006**, *6* (11), 3181−3210.

(2) Carlton, A. G.; Wiedinmyer, C.; Kroll, J. H. A review of secondary organic aerosol (SOA) formation from isoprene. *Atmos. Chem. Phys.* **2009**, *9* (14), 4987−5005.

(3) Hallquist, M.; et al. The formation, properties and impact of secondary organic aerosol: Current and emerging issues. *Atmos. Chem. Phys.* **2009**, *9* (14), 5155−5236.

(4) Weber, R. J.; et al. A study of secondary organic aerosol formation in the anthropogenic-influenced southeastern United States. *J. Geophys. Res.: Atmos.* **2007**, *112* (D13), D13302.

(5) Budisulistiorini, S. H.; et al. Real-Time Continuous Character-ization of Secondary Organic Aerosol Derived from Isoprene Epoxydiols in Downtown Atlanta, Georgia, Using the Aerodyne Aerosol Chemical Speciation Monitor. *Environ. Sci. Technol.* **2013**, *47* (11), 5686−5694.

(6) Lin, Y. H.; Knipping, E. M.; Edgerton, E. S.; Shaw, S. L.; Surratt, J. D. Investigating the influences of SO_2 and NH_3 levels on isoprene-derived secondary organic aerosol formation using conditional sampling approaches. *Atmos. Chem. Phys.* **2013**, *13* (16), 8457−8470.

(7) Paulot, F.; Crounse, J. D.; Kjaergaard, H. G.; Kürten, A.; St. Clair, J. M.; Seinfeld, J. H.; Wennberg, P. O. Unexpected Epoxide Formation in the Gas-Phase Photooxidation of Isoprene. *Science* **2009**, *325* (5941), 730−733.

(8) Lin, Y.-H.; et al. Epoxide as a precursor to secondary organic aerosol formation from isoprene photooxidation in the presence of nitrogen oxides. *Proc. Natl. Acad. Sci. U.S.A.* **2013**, *110* (17), 6718−6723.

(9) Surratt, J. D.; et al. Reactive intermediates revealed in secondary organic aerosol formation from isoprene. *Proc. Natl. Acad. Sci. U.S.A.* **2010**, *107* (15), 6640−6645.

(10) Lin, Y.-H.; et al. Isoprene Epoxydiols as Precursors to Secondary Organic Aerosol Formation: Acid-Catalyzed Reactive Uptake Studies with Authentic Compounds. *Environ. Sci. Technol.* **2012**, *46* (1), 250−258.

(11) Gaston, C. J.; Riedel, T. P.; Zhang, Z.; Gold, A.; Surratt, J. D.; Thornton, J. A. Reactive Uptake of an Isoprene-Derived Epoxydiol to Submicron Aerosol Particles. *Environ. Sci. Technol.* **2014**, *48* (19), 11178−11186.

(12) Pye, H. O. T.; et al. Epoxide Pathways Improve Model Predictions of Isoprene Markers and Reveal Key Role of Acidity in Aerosol Formation. *Environ. Sci. Technol.* **2013**, *47* (19), 11056−11064.

(13) Alexander, B.; Hastings, M. G.; Allman, D. J.; Dachs, J.; Thornton, J. A.; Kunasek, S. A. Quantifying atmospheric nitrate formation pathways based on a global model of the oxygen isotopic composition (delta(17)O) of atmospheric nitrate. *Atmos. Chem. Phys.* **2009**, *9* (14), 5043−5056.

(14) McNeill, V. F.; Woo, J. L.; Kim, D. D.; Schwier, A. N.; Wannell, N. J.; Sumner, A. J.; Barakat, J. M. Aqueous-Phase Secondary Organic Aerosol and Organosulfate Formation in Atmospheric Aerosols: A Modeling Study. *Environ. Sci. Technol.* **2012**, *46* (15), 8075−8081.

(15) Bates, K. H.; Crounse, J. D.; St. Clair, J. M.; Bennett, N. B.; Nguyen, T. B.; Seinfeld, J. H.; Stoltz, B. M.; Wennberg, P. O. Gas Phase Production and Loss of Isoprene Epoxydiols. *J. Phys. Chem. A* **2014**, *118* (7), 1237−1246.

(16) Thornton, J. A.; Braban, C. F.; Abbatt, J. P. D. N_2O_5 hydrolysis on sub-micron organic aerosols: The effect of relative humidity,

particle phase, and particle size. *Phys. Chem. Chem. Phys.* **2003**, *5* (20), 4593−4603.

(17) Thornton, J. A.; Abbatt, J. P. D. N_2O_5 reaction on submicron sea salt aerosol: Kinetics, products, and the effect of surface active organics. *J. Phys. Chem. A* **2005**, *109* (44), 10004−10012.

(18) Zhang, Z.; Lin, Y. H.; Zhang, H.; Surratt, J. D.; Ball, L. M.; Gold, A. Technical Note: Synthesis of isoprene atmospheric oxidation products: Isomeric epoxydiols and the rearrangement products cis- and trans-3-methyl-3,4-dihydroxytetrahydrofuran. *Atmos. Chem. Phys.* **2012**, *12* (18), 8529−8535.

(19) Bertram, T. H.; Kimmel, J. R.; Crisp, T. A.; Ryder, O. S.; Yatavelli, R. L. N.; Thornton, J. A.; Cubison, M. J.; Gonin, M.; Worsnop, D. R. A field-deployable, chemical ionization time-of-flight mass spectrometer. *Atmos. Meas. Tech.* **2011**, *4* (7), 1471−1479.

(20) Kercher, J. P.; Riedel, T. P.; Thornton, J. A. Chlorine activation by N_2O_5: Simultaneous, in situ detection of $ClNO_2$ and N_2O_5 by chemical ionization mass spectrometry. *Atmos. Meas. Tech.* **2009**, *2* (1), 193−204.

(21) Brown, R. L. Tubular Flow Reactors With First-Order Kinetics. *J. Res. Natl. Bur. Stand. (U.S.)* **1978**, *83* (1), 1−8.

(22) Clegg, S. L.; Brimblecombe, P.; Wexler, A. S. Thermodynamic Model of the System H^+−NH_4^+−Na^+−SO_4^{2-}−NO_3^-−Cl^-−H_2O at 298.15 K. *J. Phys. Chem. A* **1998**, *102* (12), 2155−2171.

(23) Wexler, A. S.; Clegg, S. L. Atmospheric aerosol models for systems including the ions H^+, NH_4^+, Na^+, SO_4^{2-}, NO_3^-, Cl^-, Br^-, and H_2O. *J. Geophys. Res.: Atmos.* **2002**, *107* (D14), ACH 14-1−ACH 14-14.

(24) Nguyen, T. B.; et al. Organic aerosol formation from the reactive uptake of isoprene epoxydiols (IEPOX) onto non-acidified inorganic seeds. *Atmos. Chem. Phys.* **2014**, *14* (7), 3497−3510.

(25) Eddingsaas, N. C.; VanderVelde, D. G.; Wennberg, P. O. Kinetics and Products of the Acid-Catalyzed Ring-Opening of Atmospherically Relevant Butyl Epoxy Alcohols. *J. Phys. Chem. A* **2010**, *114* (31), 8106−8113.

(26) Birdsall, A. W.; Miner, C. R.; Mael, L. E.; Elrod, M. J. Mechanistic study of secondary organic aerosol components formed from nucleophilic addition reactions of methacrylic acid epoxide. *Atmos. Chem. Phys.* **2014**, *14* (23), 12951−12964.

(27) Matsunaga, A.; Ziemann, P. J. Gas-Wall Partitioning of Organic Compounds in a Teflon Film Chamber and Potential Effects on Reaction Product and Aerosol Yield Measurements. *Aerosol Sci. Technol.* **2010**, *44* (10), 881−892.

(28) Zhang, X.; Cappa, C. D.; Jathar, S. H.; McVay, R. C.; Ensberg, J. J.; Kleeman, M. J.; Seinfeld, J. H. Influence of vapor wall loss in laboratory chambers on yields of secondary organic aerosol. *Proc. Natl. Acad. Sci. U.S.A.* **2014**, *111* (16), 5802−5807.